

USING ORBITAL EFFECTS TO BREAK THE CLOSE/WIDE DEGENERACY IN BINARY-LENS MICROLensing EVENTS

I.-G. SHIN⁰⁰¹, T. SUMI^{101,100}, A. UDALSKI^{201,200}, J. Y. CHOI⁰⁰¹, C. HAN^{001,900}, A. GOULD³⁰¹

AND

F. ABE¹⁰², D. P. BENNETT¹⁰³, I. A. BOND¹⁰⁴, C. S. BOTZLER¹⁰⁵, P. CHOTE¹⁰⁶, M. FREEMAN¹⁰⁵, A. FUKUI¹⁰⁷, K. FURUSAWA¹⁰², P. HARRIS¹⁰⁶, Y. ITOW¹⁰², C. H. LING¹⁰⁴, K. MASUDA¹⁰², Y. MATSUBARA¹⁰², N. MIYAKE¹⁰², Y. MURAKI¹⁰⁸, K. OHNISHI¹⁰⁹, N. RATTENBURY¹⁰⁵, TO. SAITO¹¹⁰, D. J. SULLIVAN¹⁰⁶, D. SUZUKI¹⁰¹, W. L. SWEATMAN¹⁰⁴, P. J. TRISTRAM¹¹¹, K. WADA¹⁰¹, P. C. M. YOCK¹⁰⁵

(THE MOA COLLABORATION),

M. K. SZYMAŃSKI²⁰¹, M. KUBIAK²⁰¹, I. SOSZYŃSKI²⁰¹, G. PIETRZYŃSKI^{201,202}, R. POLESKI²⁰¹, K. ULACZYK²⁰¹, P. PIETRUKOWICZ²⁰¹, S. KOZŁOWSKI²⁰¹, J. SKOWRON³⁰¹, AND Ł. WYRZYKOWSKI^{201,203}

(THE OGLE COLLABORATION)

⁰⁰¹Department of Physics, Institute for Astrophysics, Chungbuk National University, Cheongju 371-763, Korea

¹⁰¹Department of Earth and Space Science, Osaka University, Osaka 560-0043, Japan

²⁰¹Warsaw University Observatory, Al. Ujazdowskie 4, 00-478 Warszawa, Poland

³⁰¹Department of Astronomy, Ohio State University, 140 W. 18th Ave., Columbus, OH 43210, USA

¹⁰²Solar-Terrestrial Environment Laboratory, Nagoya University, Nagoya, 464-8601, Japan

¹⁰³Department of Physics, University of Notre Dame, Notre Dame, IN 46556, USA

¹⁰⁴Institute of Information and Mathematical Sciences, Massey University, Private Bag 102-904, North Shore Mail Centre, Auckland, New Zealand

¹⁰⁵Department of Physics, University of Auckland, Private Bag 92019, Auckland, New Zealand

¹⁰⁶School of Chemical and Physical Sciences, Victoria University, Wellington, New Zealand

¹⁰⁷Okayama Astrophysical Observatory, National Astronomical Observatory, 3037-5 Honjo, Kamogata, Asakuchi, Okayama 719-0232, Japan

¹⁰⁸Department of Physics, Konan University, Nishiokamoto 8-9-1, Kobe 658-8501, Japan

¹⁰⁹Nagano National College of Technology, Nagano 381-8550, Japan

¹¹⁰Tokyo Metropolitan College of Industrial Technology, Tokyo 116-8523, Japan

¹¹¹Mt. John Observatory, P.O. Box 56, Lake Tekapo 8770, New Zealand

²⁰²Universidad de Concepción, Departamento de Astronomía, Casilla 160-C, Concepción, Chile

²⁰³Institute of Astronomy, University of Cambridge, Madingley Road, Cambridge CB3 0HA, United Kingdom

¹⁰⁰The MOA Collaboration

²⁰⁰The OGLE Collaboration and

⁹⁰⁰Corresponding author

Draft version December 17, 2012

ABSTRACT

Microlensing can provide an important tool to study binaries, especially those composed of faint or dark objects. However, accurate analysis of binary-lens light curves is often hampered by the well-known degeneracy between close ($s < 1$) and wide ($s > 1$) binaries, which can be very severe due to an intrinsic symmetry in the lens equation. Here s is the normalized projected binary separation. In this paper, we propose a method that can resolve the close/wide degeneracy using the effect of a lens orbital motion on lensing light curves. The method is based on the fact that the orbital effect tends to be important for close binaries while it is negligible for wide binaries. We demonstrate the usefulness of the method by applying it to an actually observed binary-lens event MOA-2011-BLG-040/OGLE-2011-BLG-0001, which suffers from severe close/wide degeneracy. From this, we are able to uniquely specify that the lens is composed of K and M-type dwarfs located at ~ 3.5 kpc from the Earth.

Subject headings: gravitational lensing: micro – binaries: general

1. INTRODUCTION

Currently, about 2000 microlensing events are being detected each year from survey experiments (OGLE: Udalski 2003; MOA: Bond et al. 2001; Sumi et al. 2003). Among them, a considerable fraction are produced by objects composed of two masses. When a lensing event is produced by a binary object, the resulting light curve deviates from the smooth and symmetric form of a single-lens event (Mao & Paczyński 1991). Analyzing a binary-lens light curve is important because it enables to extract information about the lens. For general binary-lens events, this information includes the binary mass ratio, q , and the projected separation between the lens components normalized by the angular Einstein radius θ_E of the lens, s (normalized projected separation). For events with resolved caustic crossings, it is possible

to measure or constrain the mass and distance to the lens. Not being dependent on the lens luminosity, microlensing provides an important tool especially for the study of binaries composed of faint or dark objects.

However, accurate analysis of a binary-lens light curve is often hampered by the ambiguity in fits of observed light curves. Many cases of degenerate solutions are accidental, implying that the degeneracy can be resolved by precise and dense coverage of light curves. However, due to a symmetry in the lens equation itself, degeneracies between close ($s < 1$) and wide ($s > 1$) binaries can be very severe. This was first pointed out for a special case of low-mass (planetary) companions by Griest & Safazadeh (1998). It was then generalized to all binaries by Dominik (1999) and analyzed still more thoroughly by An (2005). Therefore, devising a method

resolving the close/wide degeneracy is important to uniquely characterize binary lens systems.

In this paper, we propose a method that can resolve the close/wide degeneracy. The method is based on the fact that orbital motion tends to be important for close binary lenses while it is negligible for wide binary lenses. We demonstrate the usefulness of the method in the interpretation of an actually observed lensing event MOA-2011-BLG-040/OGLE-2011-BLG-0001.

2. DEGENERACY AND RESOLUTION

The existence of an additional lens component can make lensing light curves greatly different from that of a single-lens event. The most dramatic feature of binary lensing is caustics, which represent positions on the source plane where the lensing magnification of a point source becomes infinite (Schneider & Weiß 1986). As a result, binary-lens light curves resulting from caustic-crossing source trajectories exhibit characteristic spikes. Binary lensing caustics form a single or multiple sets of closed curves each of which is composed of concave curves that meet at cusps. The caustic topology is broadly classified into three categories depending on the binary separation (Erdl & Schneider 1993). For a resonant binary with a normalized separation similar to the Einstein radius of the lens ($s \sim 1$), a single large caustic with six cusps forms around the center of mass of the binary. For a wide binary, there exist two four-cusp caustics each of which is located close to each lens components. For a close binary, there are three caustics with one four-cusp caustic located near the barycenter of the binary while the other two three-cusp caustics are located away from the center of mass.

The close/wide degeneracy in the interpretation of a binary-lens light curve occurs due to the similarity in shape between the central caustic of a close binary and either caustic of a wide binary (Albrow et al. 2001). The binary-lens parameters of the pair of degenerate close/wide binaries are related by

$$q_w = q_c(1 - q_c)^{-2} \quad (1)$$

and

$$s_w = s_c^{-1}(1 + q_c)(q_c^2 - q_c + 1)^{-1/2}, \quad (2)$$

where (s_c, q_c) and (s_w, q_w) represent the projected separations and the mass ratios of the degenerate sets of the close and wide binaries, respectively (Albrow et al. 2002). In the present context, it is important to emphasize that the degeneracy becomes especially severe when the normalized separation is either substantially smaller ($s \ll 1$) or larger ($s \gg 1$) than the Einstein radius (Shin et al. 2012).

The existence of a binary companion additionally affects lensing light curves due to the orbital motion of the binary (Albrow et al. 2000; Penny et al. 2011; Shin et al. 2011; Skowron et al. 2011). The effect of the orbital motion is twofold. First, it makes the projected binary separation vary in time, causing the shape and size of a caustic to vary during the event. Second, it also causes the projected binary axis to rotate with respect to the source trajectory, which is equivalent to the lens-source relative motion deviating from rectilinear.

The orbital effect of a binary lens can provide a useful tool that allows one to resolve the close/wide degeneracy. The physical Einstein radius of a typical Galactic bulge event is $\sim 1 - 2$ AU. Then, orbital periods of wide binaries would be substantially longer than a year. Considering that typical durations of binary-induced deviations are of order of 10 days, then, the orbital effect on the light curve of a wide binary event

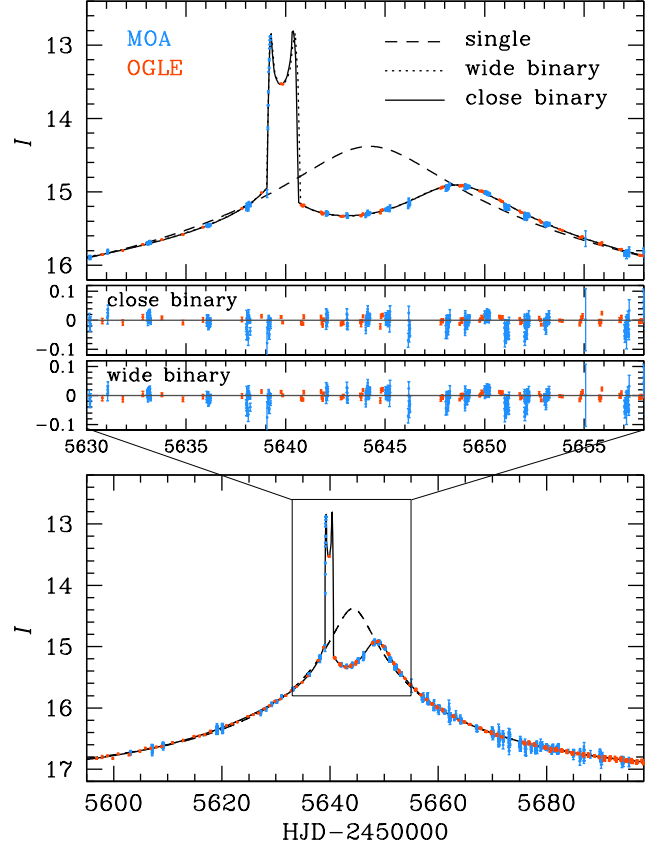


FIG. 1.— Light curve of MOA-2011-BLG-040/OGLE-2011-BLG-0001. Also drawn are the best-fit curves based on single-lens, wide-binary, and close-binary lens models. We note that the close and wide-binary models are too degenerate to be visually distinguished.

would be negligible. By contrast, orbital periods of close binaries can be small and thus the change of the lens position caused by the orbital motion during the deviating part of a lensing event can be important for some close binary events. Hence, if it is found that the orbital effect is needed to describe an observed light curve, the close binary interpretation would be the correct one between two the possible close/wide binary interpretations. On the other hand, if the orbital motion is constrained to be extremely small, this would not absolutely rule out the close-binary solution, because the projected separation of a binary with a large semi-major axis can be small when the binary axis is aligned with the line of sight. However, because such extreme projections are a priori unlikely, strong upper limits on orbital motion would statistically favor wide solutions.

3. DEMONSTRATION

We apply the orbit-based method of resolving the close/wide binary degeneracy to an actually observed event MOA-2011-BLG-040/OGLE-2011-BLG-0001. The event was discovered from the survey conducted by the Microlensing Observations in Astrophysics (MOA) group on 2011-Mar-12 toward the Galactic bulge at $(\alpha, \delta)_{J2000} = (17^h54^m00^s.02, -29^\circ06'05''.70)$, i.e., $(l, b) = (0.799^\circ, -1.657^\circ)$, based on observation using the 1.8 m telescope at Mt. John observatory in New Zealand (Sumi et al. 2011). The event was also independently discovered in May 2011 by the Optical Gravitational Lensing Experiment (OGLE), immediately after commissioning of the Early

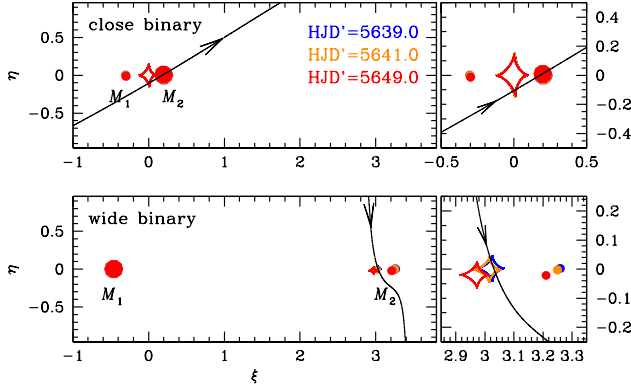


FIG. 2.— Geometry of the lens systems corresponding to the close (upper panel) and wide-binary (lower panel) solutions. In each panel, the cuspy figures indicate the caustics at the times marked in the upper panel. The dots marked by M_1 and M_2 represent the binary components, where the bigger dot represents the heavier component. The curve with an arrow represents the source trajectory. Right panels show enlargements of the region around the caustic where the deviation occurred. The coordinates (ξ, η) are centered at the center of mass of the binary and all lengths are scaled by the angular Einstein radius corresponding to the total mass of the binary lens. The ξ -axis is set as the binary axis at the time $\text{HJD}' = \text{HJD} - 2450000 = 5640.0$.

Warning System (EWS) of microlensing event detections (Udalski 2003) for OGLE-IV phase. OGLE-IV has been conducted since March 2010 with the 1.3 m Warsaw telescope and 32 CCD detector mosaic camera at Las Campanas Observatory in Chile. Reductions of data were processed using photometry codes developed by the individual groups.

Figure 1 shows the light curve of MOA-2011-BLG-040/OGLE-2011-BLG-0001. It exhibits a deviation from the unperturbed single-lens light curve near the peak. The deviation is composed of multiple features. One at $\text{HJD}' (= \text{HJD} - 2450000) \sim 5639$, shows a typical caustic-crossing feature of a strong spike. Another feature is the bump at $\text{HJD}' \sim 5649$. Located between the two features is an extended negative deviation region that lasted for ~ 6 days.

In modeling the light curve of the event, we search for a solution of lensing parameters that best describes the observed light curve. For the basic description of a binary-lens light curve, seven lensing parameters are needed. The first three describe the relative lens-source motion, including the time of the closest of the source star approach to the center of mass of the binary lens, t_0 , the lens-source separation at that moment, u_0 , and the time scale for the source to cross the Einstein radius, t_E (Einstein time scale). Another three parameters are related to the binary nature of the lens, including the normalized projected binary separation, s , the mass ratio between the binary components, q , and the angle between the source trajectory and the binary axis, α . The last parameter is $\rho_* = \theta_*/\theta_E$, the angular source radius θ_* normalized by the angular Einstein radius. The normalized source radius ρ_* is needed to account for the finite-source effect which affects lensing magnifications during caustic crossings or approaches. With these parameters, the solution of the lensing parameters is searched by minimizing χ^2 in a parameter space. This is done by a combination of grid search and down-hill approach. The grid search is done in the space of the parameters (s, q, α) , which are related to features of lensing curves in a complex way. For the χ^2 minimization in the down-hill approach, we use the Markov Chain Monte Carlo method. Considering the possibility of the existence of degenerate close and wide binary solutions, the search is done in the parameter space that is wide enough to encompass both binary solutions. From this

TABLE 1
MODEL PARAMETERS

Parameter	Close	Wide
χ^2/dof	7734/7955	7856/7955
t_0 (HJD')	5642.40 ± 0.02	5587.30 ± 0.27
u_0	-0.0914 ± 0.0008	2.9765 ± 0.0084
t_E (days)	53.14 ± 0.39	130.59 ± 0.44
s_0	0.506 ± 0.002	3.718 ± 0.007
q	1.502 ± 0.013	0.142 ± 0.002
α_0	-0.530 ± 0.002	1.447 ± 0.001
ρ_* (10^{-3})	2.15 ± 0.02	0.88 ± 0.01
$\pi_{E,N}$	-0.041 ± 0.067	-0.065 ± 0.003
$\pi_{E,E}$	0.127 ± 0.007	0.185 ± 0.004
ds/dt (yr^{-1})	-0.347 ± 0.027	-2.040 ± 0.019
$d\alpha/dt$ (yr^{-1})	1.744 ± 0.074	-0.273 ± 0.008

NOTE. — $\text{HJD}' = \text{HJD} - 2450000$. The lensing parameters t_0 and u_0 are measured with respect to the barycenter of the binary lens. The parameters s_0 and α_0 denote the binary separation and the source trajectory angle at $\text{HJD}' = 5640.0$, respectively.

search, we find a pair of degenerate close and wide binary solutions.

Although the overall shape of the observed light curve can be fitted with the basic binary lensing parameters, there are significant residuals to the fit. This gives a hint that second-order effects should be taken into account. Considering a long duration of the event, which lasted ~ 100 days, we examine the effect of the lens orbital motion and the parallax effect. The latter effect is caused by the positional change of the observer because of the Earth's orbital motion around the Sun (Gould 1992). It is known that the parallax effect results in a long-term deviation in lensing light curves similar to the effect of the binary-lens orbital motion (Batista et al. 2011) and thus we consider both effects simultaneously. To first order approximation, the lens orbital motion is described by two parameters ds/dt and $d\alpha/dt$, which represent the change rates of the normalized binary separation and the source trajectory angle, respectively. The parallax effect requires another two parameters $\pi_{E,N}$ and $\pi_{E,E}$, which are the components of the lens parallax vector π_E projected on the sky along the north and east equatorial coordinates, respectively. The direction of the parallax vector corresponds to the relative lens-source motion in the frame of the Earth at a specific time of the event. The amplitude of the parallax vector is the ratio of the size of the Earth's orbit to the Einstein radius projected on the observer plane. We find that taking account of these second-order effects significantly improves the fit for both the close and wide binary solutions.

In Figure 1, we present the model light curves on top of the observed data for both the close and wide binary solutions. The lensing parameters of the corresponding solutions are listed in Table 1. It is found that the close binary solution provides a better fit than the wide binary solution with $\Delta\chi^2 \sim 122$. However, the degeneracy is quite severe and thus it is difficult to visually distinguish the two model curves. To be noted is that the obtained lensing parameters s and q of the pair of degenerate solutions well follow the relations in equations (1) and (2), suggesting that the degeneracy is rooted in the symmetry of the lens-mapping equation. In Figure 2, we also present the geometry of the lens system corresponding to the individual solutions. For both solutions, the caustic-crossing feature of the light curve occurred when the source crossed a tip of a caustic and the bump was produced when the source approached a cusp of the caustic. The extended nega-

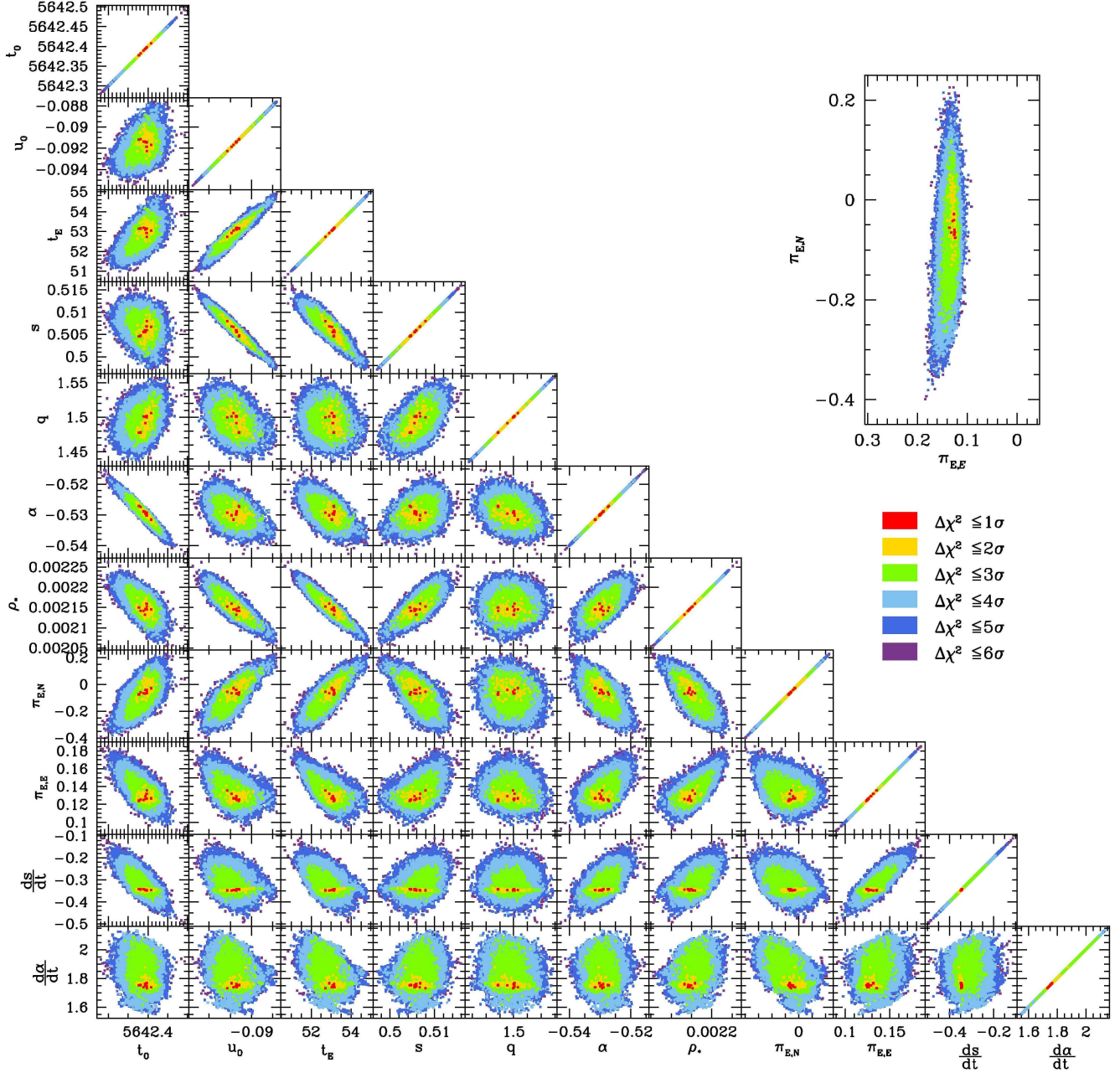


FIG. 3.— Distributions of $\Delta\chi^2$ in the space of lensing parameters. For better view, the distribution of the lens-parallax parameters, $\pi_{E,N}$ and $\pi_{E,E}$, are presented in a separate panel on the upper right corner.

tive deviation region occurred when the source passed along the fold of the caustic. Figure 3 shows $\Delta\chi^2$ distributions in the lensing-parameter spaces presented to show uncertainties and correlations between lensing parameters. The presented distributions are for the close-binary solution, which provides a better fit.

For both solutions, the orbital effect is important as indicated by the large values of the orbital parameters ds/dt and $d\alpha/dt$. According to the definition, $ds/dt = 1.0$ implies that the binary separation changes by $s = 1.0$ per year. Similarly, $d\alpha/dt = 1.0$ implies that the binary axis rotates by 1 radian per year. The obtained orbital parameters are $ds/dt = -0.35$ and $d\alpha/dt = 1.74$ for the close binary model and $ds/dt = -2.04$ and $d\alpha/dt = -0.27$ for the wide binary model. Considering that the binary-induced deviations lasted ~ 15 days, the

changes of the binary separation and the rotation angle over the course of lensing magnification are very significant for both solutions. From comparison of the model light curves obtained with and without considering the orbital effect, we find that the orbital effect is especially important for the description of the extended negative perturbation region.

The severity of the orbital effect strongly suggests that the event was produced by a close binary rather than a wide binary. For a quantitative proof of this, we evaluate the ratio of transverse kinetic to potential energy

$$\left(\frac{\text{KE}}{\text{PE}}\right)_{\perp} = \frac{(r_{\perp}/\text{AU})^3}{8\pi^2(M/M_{\odot})} \left[\left(\frac{1}{s} \frac{ds}{dt}\right)^2 + \left(\frac{d\alpha}{dt}\right)^2 \right], \quad (3)$$

which must obey $(\text{KE}/\text{PE})_{\perp} \leq \text{KE}/\text{PE}$, where KE/PE is

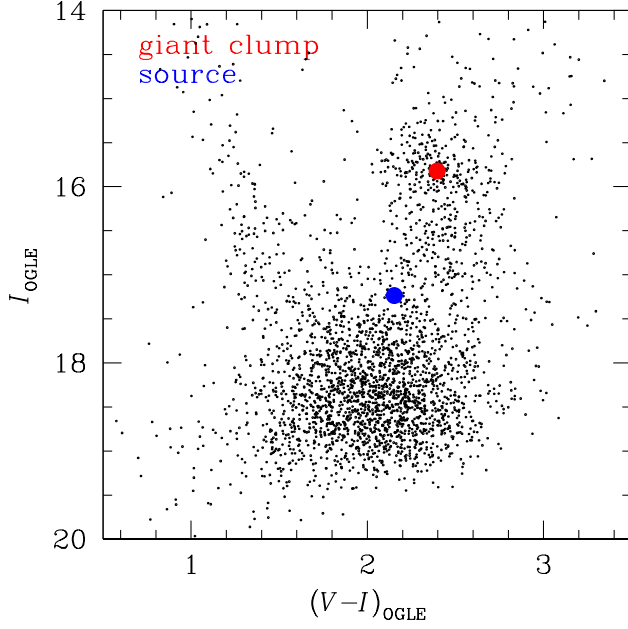


FIG. 4.— OGLE color-magnitude diagram of stars in the field where the binary-lens event MOA-2011-BLG-040/OGLE-2011-BLG-0001 occurred. The red and blue dots represent the centroid of the giant clump and the location of lensed star, respectively

the ratio of (3-dimensional) kinetic to potential energy (Dong et al. 2009). Here M is the total mass of the binary system, $r_{\perp} = sD_L\theta_E$ is the physical projected separation between the lens components, and D_L represents the distance to the lens. An energy ratio greater than unity implies that a binary system is dynamically unbound.

To determine the energy ratio, it is required to measure the total mass and distance to the lens. We determine these quantities from the measured lens parallax and the angular Einstein radius by

$$M = \frac{\theta_E}{\kappa\pi_E}, \quad (4)$$

and

$$D_L = \frac{\text{AU}}{\pi_E\theta_E + \pi_S}, \quad (5)$$

where $\pi_E = (\pi_{E,N}^2 + \pi_{E,E}^2)^{1/2}$, $\pi_S = \text{AU}/D_S$, and D_S represents the distance to the source star. The Einstein radius is measured by $\theta_E = \theta_*/\rho_*$. The normalized source radius ρ_* is determined from light curve fitting. In this process, we consider the limb-darkening variation of the source star's surface by modeling the surface-brightness profile as $S_{\lambda} = (F_{\lambda}/\pi\theta_*^2)[1 - \Gamma_{\lambda}(1 - 3\cos\psi/2)]$, where Γ_{λ} is the linear limb-darkening coefficient, F_{λ} is the source star flux, and ψ is the angle between the normal to the source star's surface and the line of sight toward the star. We adopt $\Gamma_R = 0.53$ and $\Gamma_I = 0.44$ based on the source type determined by the procedure described below. We estimate the angular source radius θ_* from the dereddened color $(V-I)_0$ and brightness I_0 using an instrumental color-magnitude diagram (Yoo et al. 2004). For the event, we estimate the instrumental color of the source based on linear regression method by using multi-band (V and I) OGLE data. Then, we measure the offset $\Delta[(V-I), I] = (-0.24, +1.41)$ of the source star from the centroid of bulge giant clump, whose dereddened position is known independently, $[(V-I), I]_{0,c} = (1.06, 14.41)$ (Bensby et al. 2011; Nataf et al. 2012). This

TABLE 2
PHYSICAL LENS PARAMETERS

Parameter	Close	Wide
$M (M_{\odot})$	$1.08^{+0.05}_{-0.24}$	1.80 ± 0.05
$M_1 (M_{\odot})$	$0.43^{+0.02}_{-0.10}$	1.58 ± 0.04
$M_2 (M_{\odot})$	$0.65^{+0.03}_{-0.14}$	0.22 ± 0.01
θ_E (mas)	1.17 ± 0.01	2.88 ± 0.02
μ (mas yr $^{-1}$)	8.04 ± 0.02	8.05 ± 0.06
D_L (kpc)	$3.54^{+0.06}_{-0.45}$	1.45 ± 0.03
$(KE/PE)_{\perp}$	$0.38^{+0.02}_{-0.05}$	9.84 ± 0.58

NOTE. — M : total mass of the close binary, M_1 and M_2 : masses of the binary components, θ_E : angular Einstein radius, μ : relative lens-source proper motion, D_L : distance to the lens, $(KE/PE)_{\perp}$: transverse kinetic to potential energy ratio.

yields the dereddened color and magnitude of the source star $(V-I)_{0,S} = (0.82, 15.79)$, indicating that the source is a low-luminosity bulge giant. Figure 4 shows the locations of the source star and the centroid of giant clump in the color-magnitude diagram constructed based on OGLE data. Once the dereddened $V-I$ color of the source star is measured, it is translated into $V-K$ color by using the $V-I$ versus $V-K$ relations of Bessell & Brett (1988) and then the angular source radius is estimated by using the relation between $V-K$ colors and angular stellar radii given by Kervella et al. (2004).

In Table 2, we list the projected kinetic to potential energy ratios for the close and wide binary solutions along with the determined physical quantities. For the close binary solution, this ratio $[(KE/PE)_{\perp} = 0.4]$ is smaller than unity, implying that the binary lens system is dynamically stable. By contrast, for the wide binary solution, this ratio $[(KE/PE)_{\perp} = 9.8]$ is much larger than unity, implying that the binary system is dynamically *unstable* and thus the wide binary cannot be the solution of the observed light curve. This demonstrates that detections of orbital effect can be used to resolve severe binary degeneracies. By resolving the degeneracy, the physical parameters of the lens are uniquely determined. The measured masses of the binary components are $0.65 M_{\odot}$ and $0.43 M_{\odot}$, which correspond to K and M-type dwarfs, respectively. The distance to the lens is ~ 3.5 kpc from the Earth.

4. SUMMARY AND CONCLUSION

We proposed a method of resolving the close/wide degeneracy in microlensing light curves using the effect of the lens orbital motion on light curves. The method is based on the fact that the orbital effect tends to be important for close binaries while it is negligible for wide binaries. We demonstrated the usefulness of the method by applying it to an actually observed lensing event MOA-2011-BLG-040/OGLE-2011-BLG-0001. From this, we were able to uniquely identify that the lens is composed of two K and M-type dwarfs located at ~ 3.5 kpc from the Earth. Considering that the orbital effect becomes more important with the decrease of the binary separation, the proposed method would be important especially in resolving binaries with very close and wide separations for which the degeneracy is very severe.

Work by C. Han was supported by the Creative Research Initiative Program (2009-0081561) of National Research Foundation of Korea. The OGLE project has received funding from the European Research Council under the European Community's Seventh Framework Programme

(FP7/2007-2013) / ERC grant agreement no. 246678. The MOA experiment was supported by grants JSPS22403003 and JSPS23340064. T.S. was supported by the grant

JSPS23340044. Y. Muraki acknowledges support from JSPS grants JSPS23540339 and JSPS19340058. A. Gould acknowledges support from NSF AST-1103471 and NASA grant NNG04GL51G.

REFERENCES

- Albrow, M. D., Beaulieu, J.-P., Caldwell, J. A. R., et al. 2000, *ApJ*, 534, 894
 Albrow, M. D., An, J., Beaulieu, J.-P., et al. 2001 *ApJ*, 549, 759
 Albrow, M. D., An, J., Beaulieu, J.-P., et al. 2002, *ApJ*, 572, 1031
 An, J. H. 2005, *MNRAS*, 356, 1409
 Batista, V., Gould, A., Dieters, S., et al. 2011, *A&A*, 529, 102
 Bensby, T., Adén, D., Meléndez, J., et al. 2011, *A&A*, 533, 134
 Bessell, M. S., & Brett, J. M. 1988, *PASP*, 100, 1134
 Bond, I. A., Abe, F., Dodd, R. J., et al. 2001, *MNRAS*, 32, D.7, 868
 Dominik, M. 1999, *A&A*, 349, 108
 Dong, S., Gould, A., Udalski, A., et al. 2009 *ApJ*, 695, 970
 Erdl, H., & Schneider, P. 1993, *A&A*, 268, 453
 Gould, A. 1992, *ApJ*, 392, 442
 Griest, K., & Safazadeh, N. 1998, *ApJ*, 500, 37
 Kervella, P., Thévenin, F., Di Folco, E., & Ségransan, D. 2004, *A&A*, 426, 297
 Mao, S., & Paczyński, B. 1991, *ApJ*, 374, L37
 Nataf, D. M., Gould, A., Fouqué, P., et al. 2012, *ApJ*, submitted
 Penny, M. T., Mao, S., & Kerins, E. 2011, *MNRAS*, 412, 607
 Schneider, P., & Weiß, A. 1986, *A&A*, 164, 237
 Shin, I.-G., Udalski, A., Han, C., et al. 2011, *ApJ*, 735, 85
 Shin, I.-G., Choi, J.-Y., Park, S.-Y., et al. 2012, *ApJ*, 746, 127
 Skowron, J., Udalski, A., Gould, A., et al. 2011, *ApJ*, 738, 87
 Sumi, T., Abe, F., Bond, I. A., et al. 2003, *ApJ*, 591, 204
 Sumi, T., Kamiya, K., Bennett, D. P., et al. 2011, *Nature*, 473, 349
 Udalski, A. 2003, *Acta Astron.*, 53, 291
 Yoo, J., DePoy, D. L., Gal-Yam, A., et al. 2004, *ApJ*, 603, 139